Microarray Analysis of Gene Expression in the Kidneys of New- and Post-Onset Diabetic NOD Mice

Karen H.S. Wilson,[1] Sarah E. Eckenrode,[1] Quan-Zhen Li,[1] Qing-Guo Ruan,[1] Ping Yang,[1] Jing-Da Shi,[2] Abdoreza Davoodi-Semiromi,[2] Richard A. McIndoe,[1] Byron P. Croker, [2,3] and Jin-Xiong She[1]

We profiled the expression of 5,760 clones from a kidney subtraction library in the kidneys of three groups of NOD mice: nondiabetic, new-onset, and long-term diabetic. A total of 27 genes had lower expression and 1 gene (Gpx3) had higher expression in the new-onset diabetic mice compared with nondiabetic control NOD mice ($P < 0.001$). Similarly, 19 of the above 27 genes and 7 additional genes had higher expression and the Gpx3 gene had lower expression in long-term diabetic mice compared with controls ($P < 0.001$). Interestingly, only three genes may be different between new-onset and long-term diabetic mice ($P < 0.0004$). These genes are from diverse functional groups, including oxidative phosphorylation, free radical neutralization, channels, pumps, lipid processing, transcription and translation machinery, protein trafficking, constitutive protein processing, and immune function. The majority of these genes fall into four signaling pathways: insulin, transforming growth factor-β, tumor necrosis factor-α, and peroxisome proliferator–activated receptor. The most significant expression change was found for the stearoyl-coenzyme A desaturase 1 (SCD1) gene ($P < 10^{-7}$). The lower expression levels of the SCD1 gene in both diabetic groups compared with controls were further confirmed by Northern blot analysis and immunohistochemistry. *Diabetes* 52:2151–2159, 2003

Diabetic nephropathy (DN) is the leading cause of end-stage renal disease in the U.S. and the largest contributor to the total cost of diabetes care. The incidence of end-stage renal disease has risen at an annual rate of 7–9% for the last decade (1), caused in part by an incomplete understanding of renal disease pathophysiology and limited therapeutic options to prevent disease progression. The development of spontaneous autoimmune diabetes in NOD mice provides a valuable model for human type 1 diabetes. Because these mice are prone to kidney complications, they are also suitable for DN studies (2). The most common diseases, such as diabetes and its complications, have a strong genetic basis as well as an environmental influence. Uncovering the genetic causes and their interaction with the environment will allow the development of novel strategies for the diagnosis, prognosis, prevention, and/or treatment of these devastating diseases. However, conventional approaches of investigation have limited the rate of progress due to the complex nature of these diseases. The recent genomic revolution has created unparalleled opportunities for biomedical research. In this study we assessed the impact of diabetes on the kidney transcriptome by comparing kidneys of a control group of nondiabetic NOD mice, a group of NOD mice at the onset of diabetes, and a group of NOD mice that had been diabetic for 1 month.

RESEARCH DESIGN AND METHODS

Animals. Mice used in this study were from the colony of the University of Florida. Diabetes was confirmed by two readings of blood glucose values >200 mg/dl. Long-term diabetic mice were on insulin therapy by subcutaneous injections of insulin (10 IU/kg) once a day.

RNA. Immediately after the mice were killed, kidneys were flash-frozen in liquid nitrogen and stored at −80°C. Total RNA was extracted using a Qiagen mini-kit, and poly(A)$^+$ RNA was purified using an Oligotex mRNA mini-kit. For histology and Northern blotting studies, the two poles from the left kidney were removed, snap-frozen, and stored at −80°C. The center one-third of the left kidney was fixed in 10% buffered formalin for routine histology and immunohistochemistry. The right kidney was first weighed and then prepared for histological evaluations.

Northern blot. Total RNA was reverse-transcribed into cDNA for PCR amplification of the stearoyl-coenzyme A desaturase 1 (SCD1) probe. The primers for the SCD1 probe are a forward primer, 5′-CAT GCT CCA AGA GAT CTC CA-3′, and a reverse primer, 5′-CAG AGC GCT GGT CAT GTA G-3′. After PCR, the probe was purified by electrophoresis, extracted from the gel, and ^{32}P-labeled with the Primeit II Stratagene Random Labeling kit. Total RNA (15 μg) was loaded on a 1.6% agarose gel containing 20% formaldehyde and 1 × MOPS. Electrophoresis was allowed to proceed for 3 h at 150 V, after which the RNA was transferred overnight onto a BrightStar membrane (Ambion) in 20 × sodium chloride–sodium citrate. After UV crosslinking and prehybridization, the filter was hybridized overnight at 42°C with the ^{32}P-labeled SCD1 probe in ultrahybe buffer (Ambion).

Histology and immunohistochemistry. Tissues were imbedded in paraffin, and 3-μm thick sections were stained with hematoxylin and eosin as well as periodic acid Schiff. Frozen tissue sections were fixed in acetone and washed with Tris buffer followed by peroxide (peroxiblock; Zymed, South San Francisco, CA) and serum and avidin blocking. Tissue sections were respectively exposed to different titers of SCD1 primary antibody (Santa Cruz Biotechnology, Santa Cruz, CA). Secondary antibody incubation and detection were performed with the ABC/DAB Elite kit (goat IgG type; Vectorlabs, Burlingame, CA) according to the manufacturer. Optimal SCD1 primary antibody titer was found to be a 1:40 dilution (2.5 μg/ml). Immunohistochemistry with SCD1 was conducted on paraffin sections. The tissue sections were deparaffinated in xylene and washed with 100% ethanol. Endogenous peroxi-

From the [1]Center for Biotechnology and Genomic Medicine, Medical College of Georgia, Augusta, Georgia; the [2]Department of Pathology, Immunology and Laboratory Medicine, College of Medicine, University of Florida, Gainesville, Florida; and the [3]North Florida/South Georgia Veterans Health System, Gainesville, Florida.

Address correspondence and reprint requests to Dr. Jin-Xiong She, Center for Biotechnology and Genomic Medicine, Medical College of Georgia, 1120 15th St., PV6B108, Augusta, GA 30912. E-mail: jshe@mail.mcg.edu.

Q.-Z.L. is currently affiliated with the Center for Immunology, University of Texas Southwestern Medical Center, Dallas, Texas.

Received for publication 7 March 2003 and accepted in revised form 22 April 2003.

aadUTP, 5-(3-aminoallyl)-2′-deoxyuridine 5′-triphosphate; DN, diabetic nephropathy; ODC, ornithine decarboxylase; PPAR, peroxisome proliferator–activated receptor; SCD1, stearoyl-coenzyme A desaturase 1; SOD-1, superoxide dismutase 1; TGF-β, transforming growth factor-β; TZD, thiazolidinadione.

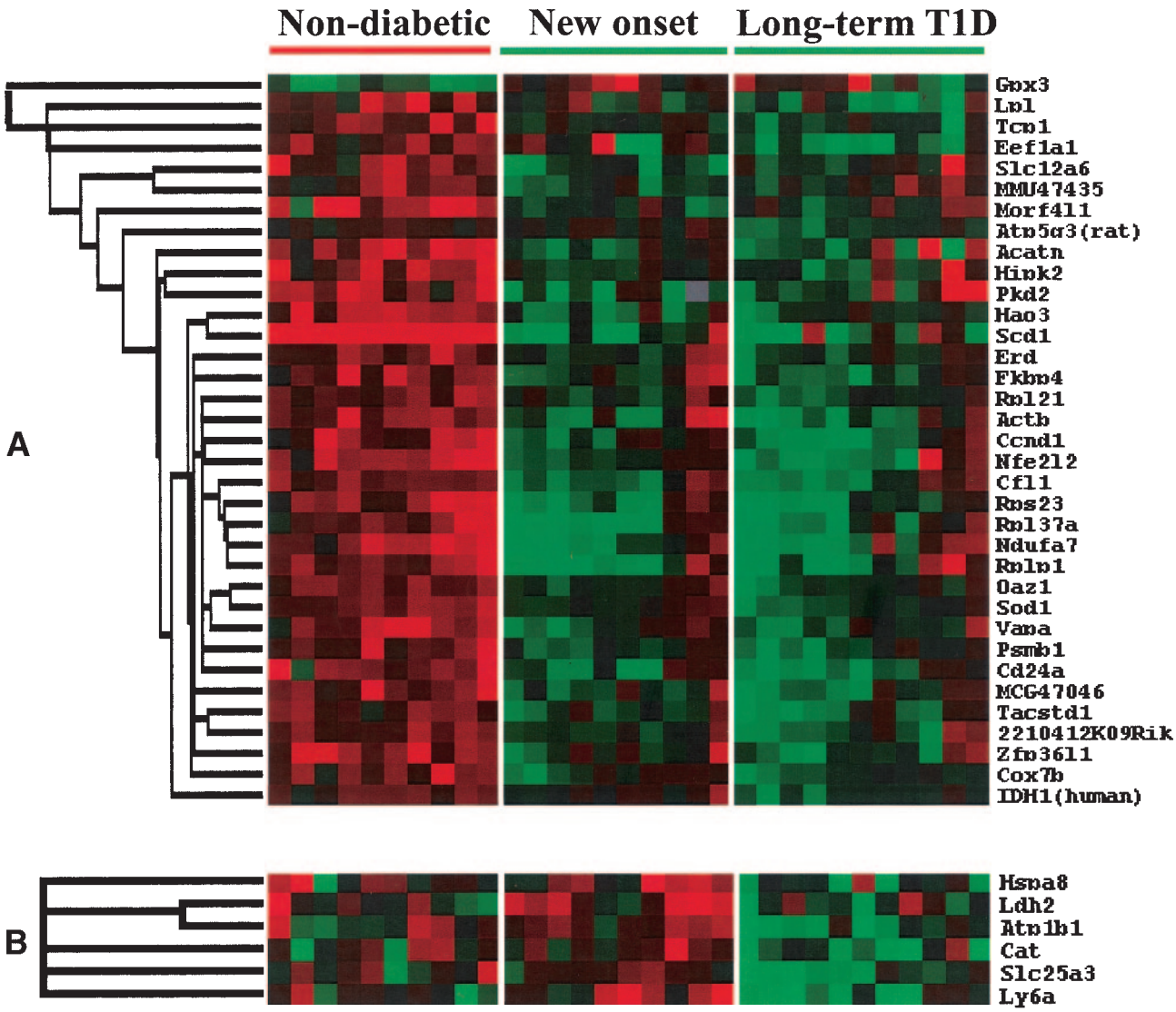

FIG. 1. Gene expression profiles in the kidneys. Each column represents one mouse, and the color bars represent the median value of three array experiments for an individual mouse for that gene. *A*: Genes differentially expressed between nondiabetic mice versus new-onset and 1-month post-onset diabetic mice. *B*: Gene expression profiles in kidneys for genes differentially expressed between new-onset and long-term diabetic mice.

dase activity was blocked with 3% H_2O_2 in methanol for 10 min followed by hydration in graded ethanol (95 and 70%) and distilled water. In preliminary tests, antigen retrieval in Trilogy (Cell Marque, Hot Springs, AK) at 95°C for 25 min, followed by standard washes, gave optimal results. Staining was comparable to the frozen sections but with better tissue structure. The tissues were then blocked with a serum/avidin solution from a Vectastain ABC/DAB Elite kit (goat IgG type; Vectorlabs). Excess serum was blotted, followed by a 1-h incubation with the SCD1 antibody at a dilution of 1:40 in diluent (Zymed) containing biotin block. The tissues were washed in Tris and incubated with biotinylated secondary anti-goat IgG antibody (Vectastain ABC/DAB Elite kit) according to the manufacturer. After washing with Tris, ABC reagent (Vectastain ABC/DAB Elite kit) followed by diaminobenzidine hydrotetrachloride chromagen (brown color) was subsequently added and washed with distilled water. The tissues were counterstained with hematoxylin, dehydrated, and mounted using Cytoseal-XYL medium (Richard-Allan Scientific).

cDNA library construction. A subtracted cDNA library was created using the PCR-Select cDNA subtraction system (CloneTech, Palo Alto, CA). Briefly, 2 μg of "diabetic" poly(A)+ mRNA (pooled mRNAs from five diabetic mice at 17–19 weeks) was used as the tester and 2 μg of "nondiabetic" poly(A)+ mRNA (pooled mRNA from five nondiabetic mice at 4 weeks) was used as the driver. The amplified fragments were then ligated into the pCR2.1 vector (Invitrogen, Carlsbad, CA), and a cDNA library was prepared in *Escherichia coli* INV F' cells.

Microarrays. The basic procedure for creating cDNA microarrays contains four major steps: amplification of cDNA clones, array printing, hybridization, and data acquisition and analysis. Details of the procedure can be found online at http://www.genomics.mcg.edu/microarray/.

Amplification of cDNA clones. A total of 5,760 cDNA clone inserts were directly PCR-amplified from 2 μl bacterial culture. The optimized 100-μl PCR was performed using a primer pair complementary to the library vector on sequences adjacent to the insert cloning sites. Primers were as follows: TAF, 5′-CCG CCA GTG TGA TGG ATA TCT G-3′; and TAR, 5′-TCC ACT AGT AAC GGC CGC CAG-3′. The PCR products were then purified by ethanol precipitation, resuspended in 25 μl of sodium phosphate buffer/SDS (150 mmol/l; pH 8.5/0.01%), and stored at −20°C until needed for printing.

Printing slides. The glass slides used in the production of the arrays were coated in-house with poly-L-lysine using a standard protocol. Purified PCR products were spotted onto the poly-L-lysine–precoated slides. The post-processing of the microarrays after printing follows the description by the Brown laboratory (available online at http://cmgm.stanford.edu/pbrown/protocols). The microarrays were then stored for up to several months in a dehumidified chamber.

Probe preparation and hybridization. The reference RNA was a pool that combines equal quantities of total RNA from the kidneys of eight nondiabetic mice at 10 weeks. RNAs were converted to cDNA and labeled with fluorophores. The reference pool cDNA was labeled with Cy5, and each experimen-

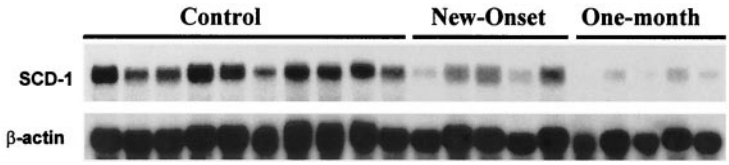

FIG. 2. Northern blot analysis for SCD1. The Northern blot membrane contains total RNA from nondiabetic NOD mice (*lanes 1–10*), new-onset diabetic NOD mice (*lanes 11–15*), and 1-month diabetic NOD (*lanes 16–20*). All mice used in the Northern blot analyses were not used in the microarray studies.

tal sample of cDNA was labeled with Cy3. The labeling of cDNA was achieved by an amino-allyl coupling strategy (3). Briefly, an amino-allyl–modified dUTP [5-(3-aminoallyl)-2′-deoxyuridine 5′-triphosphate (aadUTP)] was incorporated during cDNA synthesis from the RNA template (15 μg) in a reverse transcriptase reaction using Superscript II reverse transcriptase. After the synthesis, a monofunctional NHS-ester Cye dye (either Cy5 or Cy3; Amersham) was coupled to the modified dUTP in a sodium bicarbonate buffer. After coupling the Cye dye to the aadUTP, the unincorporated dyes were removed using a Qia-quick PCR purification kit.

Hybridization. Each Cy3-labeled probe was combined to an equal quantity of the universal Cy5-labeled reference and hybridized to a microarray. The hybridization was accomplished under a cover slip in a hybridization chamber (Array-It) and allowed to anneal for 16 h at 60°C. Slides were then washed and spun-dried.

Data acquisition. A GMS 418 Scanner (Affymetrix, Santa Clara, CA) was used to scan the images by scanning the slide twice, the first time at 532 nm and the second time at 635 nm. This process generates two 16-bit tagged image file format (TIFF) image files. Numerical values for each spot were extracted from the images using either Scanalyze by Michael Eisen (4) or Molecularware (Molecularware, Cambridge, MA).

A statistical program was used to identify/flag spots with low-intensity/background ratios (5). This flagging procedure allows us to *1*) determine whether the data quality for each spot (gene) was sufficiently good to warrant subsequent analyses and *2*) eliminate unreliable elements with expression statistically too close to the background. After "flagging," the data were uploaded to a flat file database, where the gene expression information was linked to the coordinates of the spot on the array.

Statistical and cluster analyses. Because hybridizations were repeated three times for each RNA sample to improve the accuracy of the measurements, the median of the log (2) of expression ratios from replicates were calculated for each RNA sample using Microsoft Excel 97 SR2. Subsequent statistical analyses were based on the median expression data. We used Student's t test (6) to select genes with the highest discrimination power between two groups of samples. Interesting genes were clustered using Cluster software (4) and viewed using TreeView (4).

RESULTS

Impact of diabetes on gene expression in the kidney. To assess early changes in gene expression occurring at the onset of diabetes, 10 nondiabetic NOD mice (30- to 33-week-old females) were compared by microarray analysis with 10 diabetic NOD mice (14- to 30-week-old females) at the onset of the disease. The expression profile of each RNA sample was determined in three replicates, and the median expression levels from the three replicates were used in the statistical analyses. The vast majority of the 5,760 clones spotted on the arrays were relatively constant across the two groups. Nevertheless, t tests enabled the identification of clones that are differentially expressed in the two groups of animals. Using the selection criterium of $P \leq 10^{-3}$, followed by sequencing of the relevant clones, 28 unique genes were identified. These genes were clustered using hierarchical clustering analyses (Fig. 1*A*). Of the 28 unique genes, 27 were downregulated in the new-onset diabetic mice, and only 1 gene (*Gpx3*) was upregulated (Table 1).

Impact of long-term diabetes on kidney gene expression. We also analyzed the expression profiles of 11 NOD mice that had been diabetic and on insulin therapy for 1 month (22- to 25-week-old female NOD). By using the same selection criterion as in the previous comparison ($P \leq 10^{-3}$), 26 unique genes were found to differ in expression between the long-term diabetic mice and the controls (Fig. 1*A* and Table 1). Similar to the new-onset diabetic mice, only *Gpx3* was upregulated in the long-term diabetic mice (Table 1). Among the 25 upregulated genes in the long-term diabetic group, 19 genes were also found in the comparison between nondiabetic and new-onset diabetic mice, whereas 7 genes were selected from the comparison between the long-term diabetic and control groups (Table 1). Furthermore, five of these seven genes were also different between the controls and new-onset diabetic mice, although statistical significance did not reach the threshold of $P < 0.001$. The similarity between the data from the two diabetic mouse groups versus the normal controls provides further support for our microarray data.

Interestingly, when the new-onset and long-term diabetic groups were compared, only three genes reached the statistical threshold of $P < 0.001$ (Fig. 1*B* and Table 1). Even after we relaxed the statistical criteria, only three other genes had a P value of 0.007–0.001 (Table 1).

Expression of the SCD1 gene and protein in NOD kidneys. The SCD1 gene (*Scd1*) encodes a key enzyme in the control of membrane fluidity and lipid metabolism. This gene had the most discriminating power between the diabetic and nondiabetic mice ($P < 10^{-7}$). Our microarray revealed that *Scd1* was downregulated by 3.8-fold in the new-onset diabetic mice and by 4.3-fold in the long-term diabetic mice compared with the control NOD mice. Northern blotting on a separate set of animals that were not used in microarray analysis provided confirmatory evidence for the differential gene expression data from microarray (Fig. 2). The mean expression and SD for the control, new-onset, and long-term diabetic group is 10.2 ± 5.8, 4.1 ± 2.1, and 1.0 ± 0.8, respectively. This represents a 2.5- and 10-fold decrease in the new-onset and long-term diabetic groups compared with controls, consistent with the microarray data.

Immunohistochemistry assays with an SCD1 antibody were used to localize SCD1 protein in the kidney. Previous studies have demonstrated that SCD1 is abundantly expressed in adipose tissue (7). *Scd1* mRNA has also been detected in the skin, where in situ hybridization showed that the enzyme was expressed in the sebaceous glands (8). We first tested the antibody on the C57BL/6 kidney, skin, and other organs. As shown in Fig. 3*A–D*, the sebaceous glands darkly stain as well as the adipose tissue. C57BL/6 kidney showed unstained glomerulus and vasculature. There was mild staining of the proximal tubule in a basolateral distribution. The thin limb showed no-to-minimal staining. The strongest staining was seen in the distal tubule beginning with the distal straight tubule (thick ascending limb) in a basolateral distribution. One exception was the macula densa, which showed minimal staining. The extent of staining also decreased from the

TABLE 1
Mean expression difference between nondiabetic, new-onset diabetic, and 1-month diabetic mice

Gene name	Accession ID	Functional group	Regulatory proteins
New onset versus control			
Scd1 (stearoyl-coenzyme A desaturase)	NM_009127	Lipid desaturase	TGF-β, Insulin, PPAR-γ
Gpx3 (glutathione peroxidase 3)	NM_008161	Antioxidant	TGF-β, TNF-α, PPAR-γ, GH
Nfe212 (NF-E2 related factor 2)	NM_010902	Transcription antioxidant	Antioxidant
Tcp1 (t-complex polypeptide 1)	NM_013686	Actin tubulin folding	IL3
Slc12a6 (solute carrier family 12, member 6)	NM_133648	Solute carrier	TNF-α
MMU47435 (mouse mitochondrial DNA type 6)	U47435		
Hao3 (hydroxyacid oxidase 3)	NM_019545	Hydroxy-acid oxidation	
Rplp1 (ribosomal protein large P1)	NM_018853	Ribosomal protein	
2210412K09Rik (Riken cDNA 2210412K09)	NM_029814		
Ndufa7 (NADH dehydrogenase [ubiquinone] 1α subcomplex)	NM_023202	Oxidative phosphorylation	TGF-β
Pkd2 (polycystic kidney disease 2)	NM_008861	Channel	
Rp137a	NM_009084	Ribosomal protein	
Hipk2	NM_010433		
Acatn (acetyl-coenzyme A transporter)	NM_015728	Ganglioside O-acetylation	
Morf411 (mortality factor 4 like 1)	NM_024431		
Psmb1 (proteasome subunit β type 1)	NM_011185	Protease	
Rps23 (ribosomal protein S23)	NM_024175	Ribosomal protein	
Vapa (vesicle-associated membrane protein associated protein A)	NM_013933		
Cfl1 (cofilin 1)	NM_007687	Actin polymerization	
Tacstd1 (tumor-associated calcium signal transducer 1)	NM_008532		
Cd24a	NM_009846	Immunity	
Sod1 (superoxide dismutase 1)	X06683	Antioxidant	PPAR-γ, PPAR-α, GH
Ccnd1 (cyclin D1)	NM_007631	Cell cycle G1/S	TGF-β, PPAR-γ
Zfp3611 (zinc finger protein 36, C3H type-like 1)	NM_007564	Transcript	Insulin
Rp121 (ribosomal protein L21)	NM_019647	Ribosomal protein	
Cox7b (cytochrome C oxydase subunit VIIb)	NM_025379	Oxidative phosphorylation	
MGC47046 (hypothetical protein MGC47046)	BC016415		
Oaz1 (ornithine decarboxylase antizyme)	NM_008753	Polyamine transport	Testerone
Long term versus control			
Eef1a1 (eukaryotic translation elongation factor 1 α1)	M22432	Elongation factor	EGF
Fkbp4 (FK506 binding protein 4)	X17069	Steroid receptor	
Actb (actin, β cytoplasmic)	NM_007393		
Edr (erythroid differentiation regulator)	NM_133362		
IDH1 (human) (homolog to isocitrate dehydrogenase 1 [NADP+])	NM_005896	Carbohydrate	Thyroid hormone
Atp5g3 (rat) (homolog to ATP synthase)	NM_053756	ATP synthesis	
Lpl (lipoprotein lipase)	NM_008509	Lipid, VLDL	PPAR-γ, PPAR-α, TNF-α, IFN-α
New-onset versus long-term diabetes			
Atp1b1 (ATPase, NA+/K+ transporting, β1 polypeptide)	NM_009721	Na K transport	TNF-α, IL-1α, insulin
Ly6a (lymphocyte antigen 6 complex, locus A)	NM_010738	T-cell activation	INF-γ
Slc25a3 (solute carrier family 25 [mitochondrial carrier; phosphate carrier], member 3)	NM_133668	Channel	TNF-α
Cat (catalase)	NM_009804	Antioxidant	TGF-β-1, GH
Hspa8 (heat shock protein 8)	NM_031165	Chaperone	TGF-β, PPAR-γ
Ldh2 (lactate dehydrogenase 2, B chain)	NM_008492	Anaerobic fermentation	TNF-α, IL-1

G1, nondiabetic mice; G2, new-onset diabetic; G3, 1-month diabetic; GH, growth hormone; IFN, interferon; IL, interleukin.

cortical collecting duct to the medullary collecting duct (Fig. 3*A–D*).

To verify the specificity of the antibody, the kidney tissues were stained with both antigen-blocked SCD1 antibody, nonimmune goat serum, and SCD1 antibody alone (Fig. 3). We then proceeded to studies in NOD. Figure 3 also shows results obtained with nondiabetic controls at different magnifications with or without antigen blocking. The kidney tissues exposed to blocked antibody show abrogation of staining. The assay with unblocked SCD1 antibody on control NOD gives the same general staining pattern as the B6 mouse. Decreased staining and contrast among regions are observed in the 1-month diabetic NOD (Fig. 3*E* and *F*) compared with nondiabetic NOD mice (Fig. 3*A–D*). Tubular segments are reduced in staining intensity compared with NOD control ($P < 0.005$, Wilcoxon's rank test) but have a similar relative intensity. Staining of new-onset diabetic kidneys was similar to the long-term diabetes group.

DISCUSSION

This report presents a large dataset of 93 microarrays for 31 animals and triplicate hybridizations per animal. We

TABLE 1
Continued

Ratio of mean			*P* value		
G1/G2	G1/G3	G2/G3	G1/G2	G1/G3	G2/G3
4.3	3.8	0.9	0.0000001	0.0000001	NS
0.6	0.7	1.2	0.000009	0.002	NS
1.8	2.0	1.2	0.00003	0.0002	NS
1.4	1.7	1.2	0.00003	0.003	NS
1.7	1.1	0.7	0.00005	NS	NS
1.5	1.2	0.8	0.00006	NS	0.01
1.7	1.8	1.1	0.00007	0.0002	NS
2.1	1.9	0.9	0.00007	0.003	NS
1.4	1.5	1.1	0.0001	0.0005	NS
2.1	1.9	0.9	0.0001	0.0008	NS
2.0	1.4	0.7	0.0001	NS	NS
2.0	1.7	0.9	0.0001	0.0007	NS
1.6	1.5	1.0	0.0001	0.003	NS
1.8	1.8	1.0	0.0002	0.005	NS
1.7	1.5	0.9	0.0002	0.002	NS
1.5	1.6	1.1	0.0002	0.0002	NS
1.9	2.0	1.1	0.0002	0.00003	NS
1.6	1.6	1.0	0.0003	0.00007	NS
1.5	1.6	1.0	0.0006	0.001	NS
1.4	1.6	1.1	0.0007	0.0001	NS
1.6	1.8	1.1	0.0007	0.00004	NS
1.4	1.6	1.1	0.0007	0.00008	NS
1.5	1.8	1.2	0.0008	0.00008	NS
1.5	1.7	1.1	0.0009	0.00007	NS
1.3	1.5	1.1	0.001	0.00005	NS
1.4	1.5	1.1	0.001	0.00002	NS
1.5	1.6	1.1	0.001	0.0002	NS
1.4	1.5	1.1	0.001	0.00009	NS
1.4	1.8	1.3	NS	0.00001	NS
1.4	1.6	1.2	0.01	0.00004	NS
1.5	1.9	1.2	0.008	0.0001	NS
1.3	1.4	1.1	0.009	0.0002	NS
1.2	1.4	1.2	0.02	0.0004	0.04
1.0	1.3	1.2	NS	0.0008	0.006
1.3	1.7	1.3	0.01	0.0008	NS
0.9	1.3	1.4	NS	0.009	0.0002
0.8	1.2	1.5	0.04	0.03	0.0004
1.0	1.3	1.3	NS	0.004	0.0004
0.9	1.2	1.4	NS	0.03	0.004
0.9	1.2	1.3	NS	NS	0.006
0.8	1.1	1.3	NS	NS	0.007

also applied statistical analysis to assess the significance of the microarray data. Even though we have used a fairly stringent statistical threshold ($P < 0.001$), roughly three false positives are expected from our studies (estimated based on the number of clones with reasonable intensity and used in statistical analysis). This estimation may be validated by the comparison between new-onset and long-term diabetic groups, which selected only three genes with a $P < 0.001$. Assuming that all three genes are false-positives, this number would be the estimated false-positive rate in our dataset. Therefore, we believe that the majority of the genes are truly different between the diabetic mice and normal controls, especially those genes that are differentially expressed in both diabetic groups versus controls. When interpreting the results, one should not only consider the *P* value but also previous knowledge of the gene of interest. A number of genes discovered in our study are already implicated in similar disease processes (see discussion later), and the confidence level on those genes is much higher. In addition, many differentially expressed genes may be regulated by the same factors, further increasing the confidence level on our microarray data. Even though the data may very reliable, we advocate that they should be further validated by other experimental approaches, just as we have done for one of the interesting genes (*Scd1*).

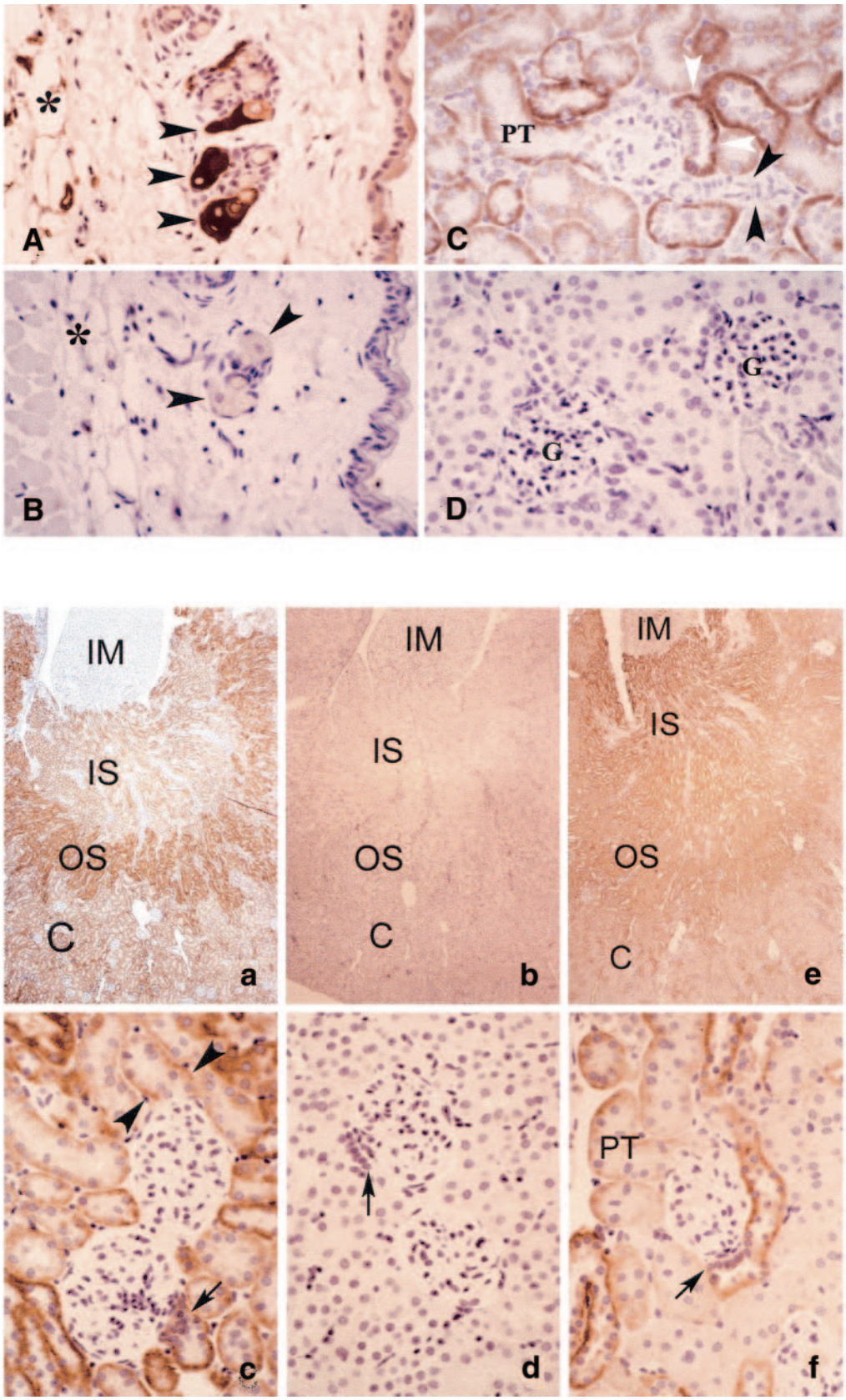

FIG. 3. SCD1 staining. *A–D*: Normal C57BL/6 mouse. *A*: Skin from C57BL/6 mouse shows sebaceous glands (arrowheads) darkly staining. Adipose tissue (*) is also stained (magnification 400×, immunoperioxidase SCD1). *B*: Skin from serial section to *A* (labeled as in *A*) shows abrogation of staining with the addition of blocking agent (400×, immunoperioxidase SCD1). *C*: C57BL/6 kidney shows unstained glomerulus (center) and afferent arteriole (dark arrowheads). Macula densa unequivocally identifies the portion of the distal tubule in the juxtaglomerular apparatus (three o'clock side of glomerulus). The distal tubule (white arrowheads) is the most dense staining region in the cortex, with the exception of the macula densa, which is sparsely stained. Several other distal tubular cross sections are present in the field. The proximal tubule (PT) arising at the tubular pole of the glomerulus (nine o'clock) and other proximal tubular cross sections show less staining than the distal tubule, but staining

One interesting finding from our study is the relatively small number of genes differentially expressed between the new-onset and long-term diabetic mice, although both diabetic groups are very different from the age-matched controls. Only three genes reached the statistical threshold of $P < 0.001$. There is also a high probability that these genes are false-positive because of the small number of genes detected in this comparison. We believe that this is less likely to have been caused by our experimental approaches. Rather, it may reflect the paucity of physiological changes between new-onset diabetic mice and those 1 month after diabetes onset. The duration of diabetes in our study may not be long enough to cause significant changes. Therefore, it will be interesting to investigate the diabetic kidneys after longer duration of diabetes.

Consistent with the high metabolic role of the kidney, genes involved in oxidative phosphorylation and ATP synthesis are changed by the presence of diabetes. A number of genes encode enzymes that protect cells against oxidative stress, whereas others were implicated in transcription and translation, lipid and carbohydrate metabolism, and the cell cycle. In addition, we found genes responsible for protein trafficking, constitutive protein processing, and immune function. Finally, a number of channels and transporters were detected by microarray analysis. A number of the genes have been previously studied in the context of type 1 diabetes. We will only discuss a few of the important groups of genes that may relate to DN.

Oxidative phosphorylation. NADH-dehydrogenase has decreased expression in the diabetic kidney. Interestingly, the activity of NADH-dehydrogenase has been reported to be significantly lower in the kidney of alloxan-induced diabetic rats (9). We found a reduced expression of cytochrome C oxidase subunit VIIb, a regulatory subunit of cytochrome C oxidase in the diabetic NOD mouse. In diabetic rats, the activity of cytochrome C oxidase has been shown to be significantly reduced in the kidneys (9).

Oxidative stress. Hyperglycemia in diabetes generates free radicals by mechanisms that are thought to involve metal-catalyzed oxidation of glucose, oxidative degeneration, and protein glycation. These observations would imply that the kidney is affected by oxidative stress. It has been suggested that enzymes normally involved in detoxifying free radicals are partially incapacitated by nonenzymatic glycosylation in diabetic individuals. Our study demonstrates that glutathione peroxidase mRNA levels are increased in the diabetic kidney of NOD mice. Consistent with this result, a number of studies have found an increase in the activity of this enzyme. Specifically, alloxan-induced (10) and streptozotocin-induced (11–14) diabetic rats have been shown to increase glutathione peroxidase activity in their kidneys when compared with controls. Other studies nevertheless suggest that the activity of glutathione peroxidase may vary during diabetes and depends on the specific location of the enzyme in the kidney. Jachec et al. (15) studied the renal cortex for glutathione peroxidase activity of streptozocin-induced diabetic rats in a time-dependent manner. The activity of glutathione peroxidase was significantly higher in diabetic rats at 5 weeks after onset of the disease. At 10 weeks of diabetes, a sharp decrease in activity was observed compared with 5 weeks, but the enzyme activity was still higher in the diabetic group. At 15 weeks, the decline in the glutathione peroxidase activity in the diabetic rats was such that it had become lower than in the controls.

In contrast to glutathione peroxidase, the expression of Cu/Zn superoxide dismutase 1 (SOD-1) was found to decline significantly in the kidneys of the diabetic NOD mouse. In agreement with this result, Genet et al. (10) noted a decrease in SOD-1 activity by 26% in the kidneys of alloxan-induced diabetic rats. Investigations with streptozotocin-induced diabetic rats, however, seem to indicate that the SOD-1 enzyme activity varies as a function of the kidney substructure and disease time course. A slight decrease in SOD-1 activity in the whole kidney was observed at 5 weeks post–diabetes onset (14), whereas others have demonstrated an increase in SOD-1 activity within 1–6 weeks after disease onset (14). Jachec et al. (15) followed SOD-1 activity over time in the diabetic rats. The observed SOD-1 activity levels in the renal cortex at 5 weeks post–diabetes onset were comparable between nondiabetic controls and diabetic rats. After 10 weeks post–diabetes onset, a slight increase in the activity of the enzyme occurred in the diabetic rats, whereas at 15 weeks post–disease onset, a decrease was observed in the diabetic rats.

Possible regulatory pathways in DN. Changes in the transcriptome or proteome during the development of DN may include functional, pathogenetic, or compensatory functions. The alterations are best understood when taken in the context of the stages of the pathological process. The time points we have studied are generally considered early in the course of DN (16–21). Nevertheless, striking hypertrophy occurs by 2 days (20,22,23) in the streptozocin model of diabetes. Rapid nephromegaly is also evident in diabetic NOD mice (2). This increase is principally caused by ornithine decarboxylase–dependent hypertrophy (19,21,23) and a subsequent increase in the activity of diverse cellular components, from NaK ATPase to transforming growth factor-β (TGF-β). In this regard, our results indicate a >30% reduction in ornithine decarboxylase (ODC)-antizyme (Oaz1) message (Table 1). This is

is also in the basolateral region (400×, immunoperioxidase SCD1). *D*: A C57BL/6 cortex with two glomeruli (G) and tubules show an abrogation of staining when the blocking agent is added (400×, immunoperioxidase SCD1). *a–f*: SCD1 staining in NOD kidneys. *a*: Survey magnification of the NOD control (nondiabetic) kidney with the cortex (C, bottom), outer stripe of the outer medulla (OS, lower center), inner stripe of the outer medulla (IS, upper center), and inner medulla (IM, top) (40×, immunoperoxidase SCD1). *b*: Serial section of NOD control kidney with abrogation of staining (labeled the same; 40×, immunoperoxidase, SCD1 with antigen blocking). *c*: 400× magnification of NOD control cortex of two glomeruli and tubules. The glomerulus at bottom shows macula densa at four o'clock (arrow) and the remainder of the distal tubule with dense basolateral staining. Other similarly stained distal tubules are seen in the field as in C57BL/6 mice. The glomerulus at top shows a tubular pole and proximal tubule at 12 o'clock with mild staining (arrowheads). *d*: NOD control serial section (same as *b*, 400×) showing two glomeruli and tubules (no staining). The macula densa is shown in the upper glomerulus (arrow). *e*: NOD diabetic kidney after 4 weeks of insulin therapy showing survey view (40×), with an overall decrease in staining and decreased contrast among the following regions: cortex (C), outer stripe (OS), inner stripe (IS), and inner medulla (IM). *f*: Higher magnification (400×) of panel *e* showing glomerulus with macula densa at one o'clock (arrow) and an associated distal tubule and tubular pole at 10–11 o'clock and an associated proximal tubule (PT). Both tubular segments are reduced in staining intensity compared with the NOD control (panel *c*, above) but have a similar relative intensity.

consistent with a complex mechanism for increased ODC activity via a double-negative regulatory mechanism involving transcriptome and proteome (24) with decreased transcription of the protein inhibitor of ODC.

In hyperglycemia, there is an increased filtered load of glucose that is reabsorbed by Na-coupled glucose transport (19,20). Secondary to Na-coupled glucose resorption, there is a decreased salt load in the distal nephron, and tubuloglomerular feedback (16) produces increased filtration (25). This response occurs within rapid physiological time (26). Although it is logical that the increased work of transport might contribute to hypertrophy, the counterintuitive events are that hypertrophy occurs before hyperfiltration. Therefore, other mechanisms, such as solute and volume shifts in the very early (<24 h) period (21) or a direct effect of glucose on the tubular epithelium (27), must initiate hypertrophy (22). Other diabetic complications of salt and volume regulation are exemplified by sodium and volume expansion exacerbated by sodium restriction (18) and hyperkalemic-hyperchloremic acidosis (17). It is this period of stable and persistent renal structural and functional abnormality that characterizes our study.

Many of the differentially expressed genes in this time period are regulated by TGF-β and peroxisome proliferator–activated receptor (PPAR) isoform signaling pathways (Table 1). TGF-β isoforms are upregulated in this early phase of diabetes, so this is an unlikely mechanism for these genes, which are downregulated (2,28) by a direct feed forward or other positive regulation (29). In contrast, a variety of metabolic effects of diabetes are linked to decreased PPAR activities. Thiazolidinadiones (TZDs) and fibrates are agonists of PPARs and correct these effects (30–32). The PPARs are potential candidates for differential downregulation of many genes in DN. We selected SCD1 for further study because it has pleotropic effects on cell membranes to lipid metabolism and may explain some of the effects seen in DN. In particular, a potential regulatory loop is suggested. The conversion of saturated long-chain fatty acids to unsaturated fatty acid is rate limiting and catalyzed by SCD1 (33). The unsaturated fatty acids are natural agonists of the PPARs (30–32), which in turn regulate SCD1. Uncertainty in completing this potential regulatory cycle appears at this point because the TZD group of PPAR agonists downregulate SCD1 in cultured preadipocites, and arachidonic acid has a similar effect in mouse liver, but SCD1 is increased in mouse skeletal muscle (34); the clofibrate type of PPAR agonists upregulate SCD1 in mouse liver (35,36). Directed studies will be important in determining kidney-specific events. Nevertheless, if the composite effect of PPAR activity is positively trophic for SCD1 in the kidney, this could produce a feedback loop in DN.

SCD1 transcription is also positively regulated by TGF-β in vitro and inhibited by overexpression of Smad7. Our study demonstrates a reduction of the FKBP class of transcripts (Table 1), which encode protein that bind and inhibit TGF-β. This is a potential mechanism for increased TGF-β signaling. Again, renal-specific effects need to be established to define the interactions of these various trophic influences. Because there is variable expression of SCD1 throughout the nephron (Fig. 3), cell-specific interactions will need to be addressed.

We discussed only a few of the potential regulatory pathways suggested by the results of this study. Nevertheless, the approach that we have taken to dissecting the kidney transcriptome in diabetes is powerful in that it reduces investigator bias in data collection and permits the concurrent analysis of a large number of genes. Certainly, it has raised more questions and provides a valuable paradigm for moving forward with this complex disease.

REFERENCES

1. Incidence & prevalence of ESRD. *Am J Kidney Dis* 38: (Suppl. 3)S37–S52, 2001
2. Sharma K, Ziyadeh FN: Renal hypertrophy is associated with upregulation of TGF-beta 1 gene expression in diabetic BB rat and NOD mouse. *Am J Physiol* 267:F1094–F1101, 1994
3. Li QZ, Eckenrode S, Ruan QG, Wang CY, Shi JD, McIndoe RA, She JX: Rapid decrease of RNA level of a novel mouse mitochondria solute carrier protein (Mscp) gene at 4–5 weeks of age. *Mamm Genome* 12:830–836, 2001
4. Eisen MB, Spellman PT, Brown PO, Botstein D: Cluster analysis and display of genome-wide expression patterns. *Proc Natl Acad Sci U S A* 95:14863–14868, 1998
5. Yang MC, Ruan QG, Yang JJ, Eckenrode S, Wu S, McIndoe RA, She JX: A statistical method for flagging weak spots improves normalization and ratio estimates in microarrays. *Physiol Genomics* 7:45–53, 2001
6. Xiong M, Jin L, Li WJ, Boerwinkle E: Computational methods for gene expression-based tumor classification. *Biotechniques* 29:1264–1268, 2000
7. Ntambi JM: The regulation of stearoyl-CoA desaturase (SCD). *Prog Lipid Res* 34:139–150, 1995
8. Zheng Y, Prouty SM, Harmon A, Sundberg JP, Stenn KS, Parimoo S: Scd3—a novel gene of the stearoyl-CoA desaturase family with restricted expression in skin. *Genomics* 71:182–191, 2001
9. Panneerselvam RS, Govindaswamy S: Effect of sodium molybdate on carbohydrate metabolizing enzymes in alloxan-induced diabetic rats. *J Nutr Biochem* 13:21–26, 2002
10. Genet S, Kale RK, Baquer NZ: Alterations in antioxidant enzymes and oxidative damage in experimental diabetic rat tissues: effect of vanadate and fenugreek (*Trigonellafoenum graecum*). *Mol Cell Biochem* 236:7–12, 2002
11. Asayama K, Yokota S, Kato K: Peroxisomal oxidases in various tissues of diabetic rats. *Diabetes Res Clin Pract* 11:89–94, 1991
12. Kakkar R, Mantha SV, Radhi J, Prasad K, Kalra J: Antioxidant defense system in diabetic kidney: a time course study. *Life Sci* 60:667–679, 1997
13. Rauscher FM, Sanders RA, Watkins JB III: Effects of coenzyme Q10 treatment on antioxidant pathways in normal and streptozotocin-induced diabetic rats. *J Biochem Mol Toxicol* 15:41–46, 2001
14. Dincer Y, Telci A, Kayali R, Yilmaz IA, Cakatay U, Akcay T: Effect of alpha-lipoic acid on lipid peroxidation and anti-oxidant enzyme activities in diabetic rats. *Clin Exp Pharmacol Physiol* 29:281–284, 2002
15. Jachec W, Tomasik A, Tarnawski R, Chwalinska E: Evidence of oxidative stress in the renal cortex of diabetic rats: favourable effect of vitamin E. *Scand J Clin Lab Invest* 62:81–88, 2002
16. Vallon V, Richter K, Blantz RC, Thomson S, Osswald H: Glomerular hyperfiltration in experimental diabetes mellitus: potential role of tubular reabsorption. *J Am Soc Nephrol* 10:2569–2576, 1999
17. Levine DZ, Iacovitti M, Burns KD: Distal tubule bicarbonate reabsorption in intact and remnant diabetic kidneys. *Kidney Int* 57:544–549, 2000
18. Miller JA, Scholey JW, Thai K, Pei YP: Angiotensin converting enzyme gene polymorphism and renal hemodynamic function in early diabetes. *Kidney Int* 51:119–124, 1997
19. Thomson SC, Deng A, Bao D, Satriano J, Blantz RC, Vallon V: Ornithine decarboxylase, kidney size, and the tubular hypothesis of glomerular hyperfiltration in experimental diabetes. *J Clin Invest* 107:217–224, 2001
20. Cortes P, Dumler F, Goldman J, Levin NW: Relationship between renal function and metabolic alterations in early streptozocin-induced diabetes in rats. *Diabetes* 36:80–87, 1987
21. Rasch R, Dorup J: Quantitative morphology of the rat kidney during diabetes mellitus and insulin treatment. *Diabetologia* 40:802–809, 1997
22. Bak M, Thomsen K, Christiansen T, Flyvbjerg A: Renal enlargement

precedes renal hyperfiltration in early experimental diabetes in rats. *J Am Soc Nephrol* 11:1287–1292, 2000
23. Seyer-Hansen K, Hansen J, Gundersen HJ: Renal hypertrophy in experimental diabetes: a morphometric study. *Diabetologia* 18:501–505, 1980
24. Oltvai ZN, Barabasi AL: Systems biology: life's complexity pyramid. *Science* 298:763–764, 2002
25. Ren Y, Garvin JL, Carretero OA: Efferent arteriole tubuloglomerular feedback in the renal nephron. *Kidney Int* 59:222–229, 2001
26. Daniels FH, Arendshorst WJ: Tubuloglomerular feedback kinetics in spontaneously hypertensive and Wistar-Kyoto rats. *Am J Physiol* 259: F529–F534, 1990
27. Ziyadeh FN, Snipes ER, Watanabe M, Alvarez RJ, Goldfarb S, Haverty TP: High glucose induces cell hypertrophy and stimulates collagen gene transcription in proximal tubule. *Am J Physiol* 259:F704–F714, 1990
28. Hill C, Flyvbjerg A, Gronbaek H, Petrik J, Hill DJ, Thomas CR, Sheppard MC, Logan A: The renal expression of transforming growth factor-beta isoforms and their receptors in acute and chronic experimental diabetes in rats. *Endocrinology* 141:1196–1208, 2000
29. Lee TI, Rinaldi NJ, Robert F, Odom DT, Bar-Joseph Z, Gerber GK, Hannett NM, Harbison CT, Thompson CM, Simon I, Zeitlinger J, Jennings EG, Murray HL, Gordon DB, Ren B, Wyrick JJ, Tagne JB, Volkert TL, Fraenkel E, Gifford DK, Young RA: Transcriptional regulatory networks in *Saccharomyces cerevisiae*. *Science* 298:799–804, 2002
30. Kliewer SA, Sundseth SS, Jones SA, Brown PJ, Wisely GB, Koble CS, Devchand P, Wahli W, Willson TM, Lenhard JM, Lehmann JM: Fatty acids and eicosanoids regulate gene expression through direct interactions with peroxisome proliferator-activated receptors alpha and gamma. *Proc Natl Acad Sci U S A* 94:4318–4323, 1997
31. Lin QO, Ruuska SE, Shaw NS, Dong D, Noy N: Ligand selectivity of the peroxisome proliferator-activated receptor alpha. *Biochemistry* 38:185–190, 1999
32. Krey G, Braissant O, L'Horset F, Kalkhoven E, Perroud M, Parker MG, Wahli W: Fatty acids, eicosanoids, and hypolipidemic agents identified as ligands of peroxisome proliferator-activated receptors by coactivator-dependent receptor ligand assay. *Mol Endocrinol* 11:779–791, 1997
33. Enoch HG, Catala A, Strittmatter P: Mechanism of rat liver microsomal stearyl-CoA desaturase: studies of the substrate specificity, enzyme-substrate interactions, and the function of lipid. *J Biol Chem* 251:5095–5103, 1976
34. Singh Ahuja H, Liu S, Crombie DL, Boehm M, Leibowitz MD, Heyman RA, Depre C, Nagy L, Tontonoz P, Davies PJ: Differential effects of rexinoids and thiazolidinediones on metabolic gene expression in diabetic rodents. *Mol Pharmacol* 59:765–773, 2001
35. Kurebayashi S, Hirose T, Miyashita Y, Kasayama S, Kishimoto T: Thiazolidinediones downregulate stearoyl-CoA desaturase 1 gene expression in 3T3-L1 adipocytes. *Diabetes* 46:2115–2118, 1997
36. Miller CW, Ntambi JM: Peroxisome proliferators induce mouse liver stearoyl-CoA desaturase 1 gene expression. *Proc Natl Acad Sci U S A* 93:9443–9448, 1996